

## Ion Density Measurement within the Equatorial Region

*K. B. Serafimov, I. S. Kutiev, J. F. Arsov, Ts. P. Dachev,  
G. A. Stanev, G. L. Gdalevich, V. V. Afonin,  
V. Gubskiy, V. Ozerov, J. Schmilauer*

### 1. Introduction

The study of electron and ion density distribution around the magnetic equator is of considerable importance in clarifying the methods of magnetic, solar-ionizing and dynamic control of the important ionospheric processes. The well-known equatorial anomaly in the latitudinal distribution of the charged particles has been the object of studies for 30 years now [1, 2, 3, 4, 5, 6, 7, 8, 10]. The investigations continue, and further regularities and specificities of this phenomenon are being discovered. For instance, the equatorial anomaly existing at altitudes of 900—1200 km during the night and the separation of crests of proton and oxygen ion concentration has been proved in [8, 9], while in [11, 12, 13] the authors have studied the irregularities in the equatorial zone by probe methods. Considerable progress is to be observed recently in the field of theoretical investigations [7, 10] and in the related phenomenon of irregular ionizing structure [13]. However, we still do not possess sufficiently reliable experimental data about the conditions of formation and disappearance of the anomaly, particularly over the region of maximal electron concentrations in the *F*-region. We do not have sufficient information about the altitudinal manifestation of this anomaly either. The lack of data on the planetary distribution of electron and ion temperatures and on their temporal changes constitutes a major difficulty for all contemporary ionospheric models. That is why, the electron and the ion concentration measurements and the electron temperature measurements performed by the Intercosmos-8 satellite whose orbit crossed the equatorial regions at various moments of the day is of considerable interest.

## II. Results from Ion Density Measurements

Ion traps described in [15, 18], Langmuir probe [16, 18], radiofrequency electron temperature probe [17], and improved electronic equipment [18] have been used on board the Intercosmos-8 satellite. This satellite performed measurements of the equatorial latitudes at geographical longitudes from 150° W to 60° E, as the transits over the magnetic equator took place at afternoon and night hours. The measurement conditions are presented in detail in Table 1.

The resulting measurements are conventionally separated into two groups, mainly from the point of view of the local time for the equatorial cross. The first group is related to the afternoon period of up to 18<sup>h</sup>30<sup>m</sup> LT and the second one is related to the night period (after 18<sup>h</sup>30<sup>m</sup> LT).

The ion concentration for the transits crossing the equator between 17<sup>h</sup>00<sup>m</sup> LT at altitudes of 308 km to 360 km under quiet magnetic conditions ( $K_p=3$ ) are presented on Fig. 1. The distributions demonstrated are typical of the day period and coincide with the data already known about the equatorial anomaly [6, 8, 9, 29]. The two characteristic minima — 15° ± 20° north and south of the equator and a clearly expressed minimum in the region of the geomagnetic equator can be seen on the Figure. A definite longitudinal effect can also be observed. In order to characterize this effect we divided the longitudinal interval into two subintervals: *A* (150° W) 70° W) and *B* (70° W, 0° W). In the first subinterval the maxima are located symmetrically to the geomagnetic equator at ±15°. In subregion *B* there exists a definite deviation from the known development of the equatorial anomaly, since the trend for the south maximum is to shift towards the equator from -15° to -5°, while the north maximum becomes considerably lower. The value of ion density in this maximum is approximately equal to the concentration of the minimum in subregion *A*. In general, the circum-equatorial distribution in subregion *B* approximates the one-maximal distribution similar to that in [27].

Fig. 2 shows characteristic data for the night group which includes the transits with local time of equatorial cross between 18<sup>h</sup>30<sup>m</sup> and 21<sup>h</sup>30<sup>m</sup>. The altitude of the equatorial cross in accordance with Table 1 is between 455 and 360 km as the satellite descends from the south to the north.

At these temporal and altitudinal conditions the general trend for the equatorial minimum is to disappear within a concentration decrease in the

Table 1  
Measurement Conditions

Geomagnetic latitude (deg.)	Local time (h)					Altitude (km)					Zenith angle (degrees)				
	Transit number					Transit number					Transit number				
	2	96	202	296	344	2	96	202	296	344	2	96	202	296	344
-50	19 <sup>h</sup> 13 <sup>m</sup>	1800	1610	1510	1455	654	608	572	502	447	79	73	57	48	43
0	21 <sup>h</sup> 34 <sup>m</sup>	2007	1828	1703	1628	455	408	360	308	267	132	114	92	73	68
50	22 <sup>h</sup> 57 <sup>m</sup>	2125	1947	1822	1750	263	245	220	209	206	157	143	125	108	106

crests (for the north one almost of one order, and for the south one — 2 to 3 times), while the concentration in the minimum almost keeps its value.

The main morphological peculiarities of subregion A are the following: in the western part ( $\lambda > 110^\circ \text{W}$ ) the main maximum is located in the south

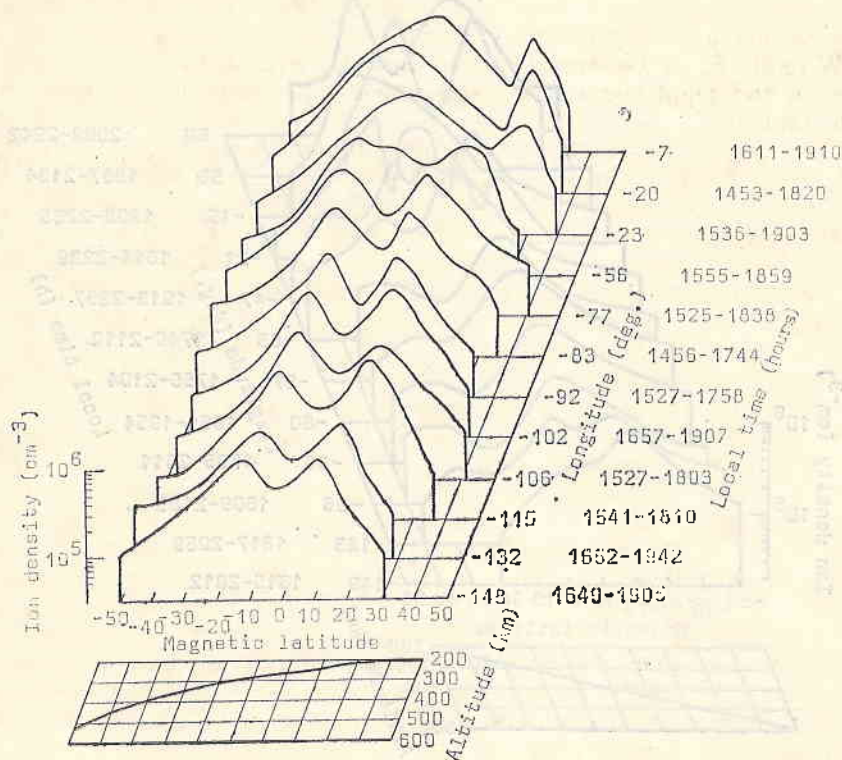


Fig. 1

hemisphere, and in the eastern part ( $\lambda < 110^\circ \text{---} 120^\circ \text{W}$ ) the main maximum is located close to the equator. The north maximum almost disappears during this period. Because of the altitudinal decrease of the orbits, the north maximum recorded in subregion B probably is due to the satellite cross through the F maximum. The main maximum in subregion B shifts from the equator to the north to  $\Phi = 15^\circ \div 20^\circ \text{N}$ . This main maximum comprises the whole latitudinal region from the equator to the designated boundary  $\Phi = 15^\circ \div 20^\circ \text{N}$ . A well expressed irregular large-scale structure is to be observed in this subregion (and especially in its western part  $-\lambda < 30^\circ \text{W}$ ). These irregularities are identified particularly in the region of the Brazilian magnetic anomaly. A similar behaviour has been described in [28], where a region between  $60^\circ \text{W}$  and  $60^\circ \text{E}$  with decreased concentration and large-scale irregularities has been sharply outlined.

At to transits between  $\lambda = 55^\circ \text{E} \div 60^\circ \text{E}$ , a well expressed bimaximal distribution of the ion concentration has been obtained. This fact shows that

the effects described in subregion *B* are of a local character and are influenced by magnetic field specificities.

The equatorial anomaly sections along the satellite orbit at day and night conditions represented here show clearly the influence of the magnetic

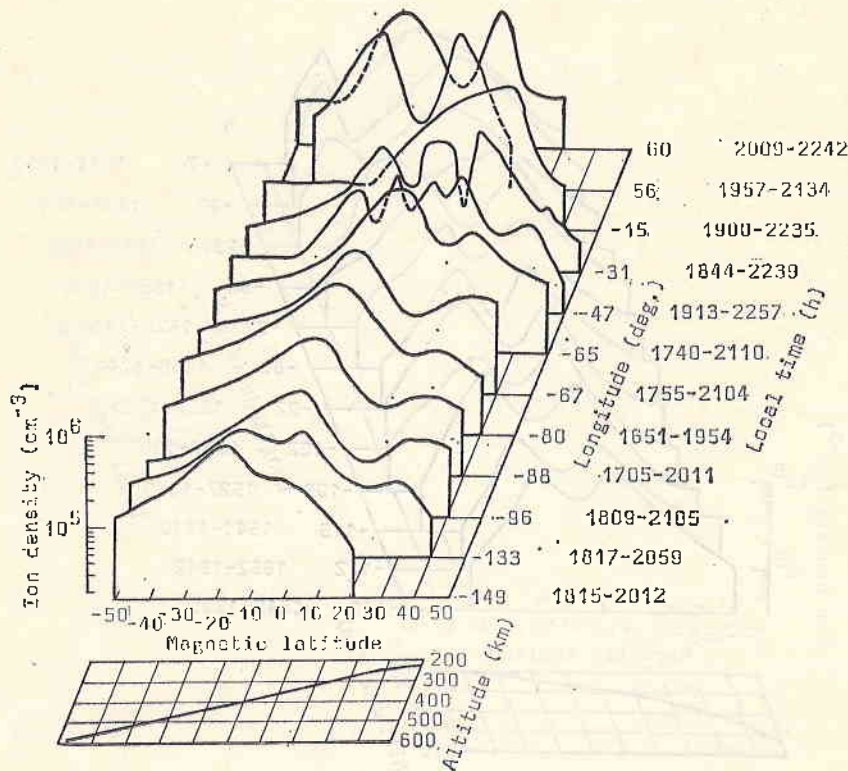


Fig. 2

field over the charged particles distribution. That can be seen particularly clear in the region of the Brazilian magnetic anomaly (about  $60^\circ$  W). By comparing Fig. 1 and Fig. 2 the conclusion is reached that the equatorial anomaly in the region under examination decays by  $19^{\text{h}}00^{\text{m}}$ . In the region of the Brazilian magnetic anomaly, strongly expressed large-scale irregularities manifest themselves after  $21^{\text{h}}00^{\text{m}}$  approximately.

### III. Electron Temperature in the Equatorial Region

Fig. 3a shows the measurement results obtained by radiofrequency electron temperature probe in the interval of geomagnetic latitudes  $\pm 40^\circ$  in quiet magnetic conditions ( $K_p < 2+$ ,  $\Sigma K_p = 10+$ ). The temperature of the neutral particles  $T_n$  close to the equator (Jacchia-71 model) are shown on the lower side of the Figure.  $T_n$ -variations at this period do not exceed  $20^\circ$  K. Data shown on Fig. 3a relate to the morning hours  $08^{\text{h}}00^{\text{m}} \div 11^{\text{h}}00^{\text{m}}$  LT, and data

in Fig. 3b relate to the night hours 20<sup>h</sup>00<sup>m</sup> ÷ 22<sup>h</sup>00<sup>m</sup> LT. Since the photoelectron flux and the electron concentration at  $\chi=85^\circ$  attain the stationary day level [25], the results shown on Fig. 3a are characteristic of daytime, and those on Fig. 3b — for the night, since  $\chi=110^\circ$ .

During 08<sup>h</sup>00<sup>m</sup> ÷ 11<sup>h</sup>00<sup>m</sup> LT (Fig. 3a) in the geomagnetic equator region there exists a deep temperature trough near the geomagnetic equator with values close to  $T_n$ .  $T_e$  smoothly decreases to its approximation of a minimum.

Even when there exists a region with  $T_e$  independent on the latitude, its latitudinal spread does not exceed several degrees. The centre of the equatorial trough is shifted to a subsolar with direction of about  $5^\circ$  from the equator. As seen from the Sun location with regard to the equatorial trough of  $T_e$ , it actually represents a geomagnetic effect. A certain asymmetry of the trough form is obviously connected with the altitudinal variation of  $T_e$  and the local time changes. At some passes  $T_e$ -variations with "amplitudes" of  $300^\circ \div 400^\circ$  K have been observed. These  $T_e$ -variations could be provoked either by kinetic effects — plasma heating and cooling at its transfer along the field lines from one hemisphere to the other [19], or by  $T_e$ -anisotropy [26]. At any rate, the minimum  $T_e$  values in the trough centre coincide with  $T_n$  in most cases, but at some passes at  $300^\circ \div 400^\circ$  K  $T_{\min}$  exceeds  $T_n$ .

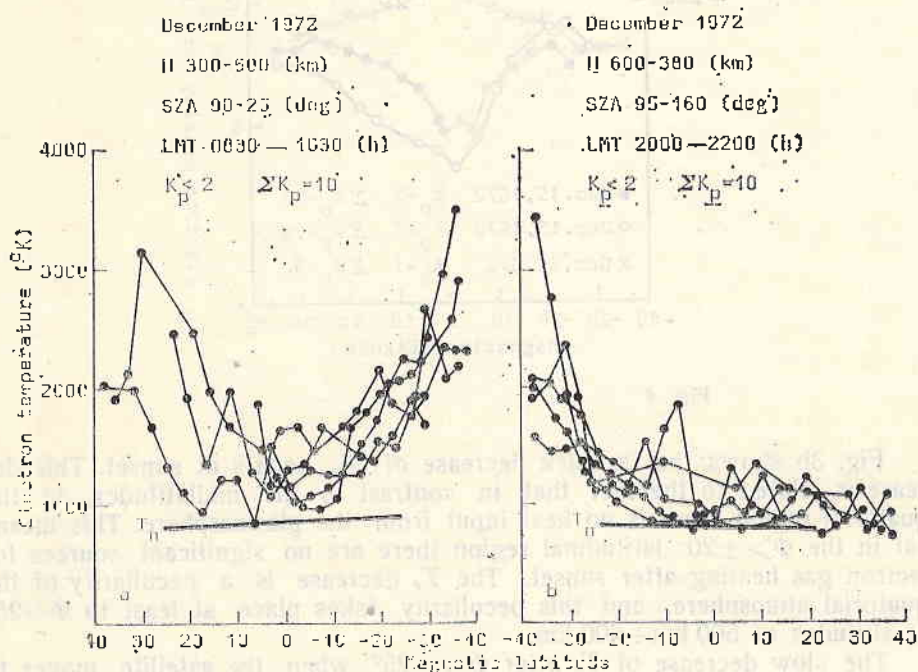


Fig. 3

Electron temperature in the trough is controlled by the ratio between the heat input and the value of  $n_i$ -concentration, which in this phase of the solar activity cycle at day is sufficiently high, for the difference between  $T_e$  and  $T_n$  should not exceed  $300^\circ \div 400^\circ$  K.

At nightfall (Fig. 3b)  $T_e$  decreases fast from  $2000^\circ \div 3000^\circ \text{K}$  at  $\Phi = -40^\circ$  to  $1200^\circ \pm 100^\circ \text{K}$  at  $\Phi = -25^\circ$ , and after that decreases monotonously to  $900^\circ \pm 100^\circ \text{K}$  at  $\Phi = -40^\circ$ . The initial fast decrease of  $T_e$  takes place during  $30^{\text{m}}$  LT. The sunset had occurred for the satellite at the represented passes in the latitudinal interval of  $20^\circ \div 30^\circ$ .

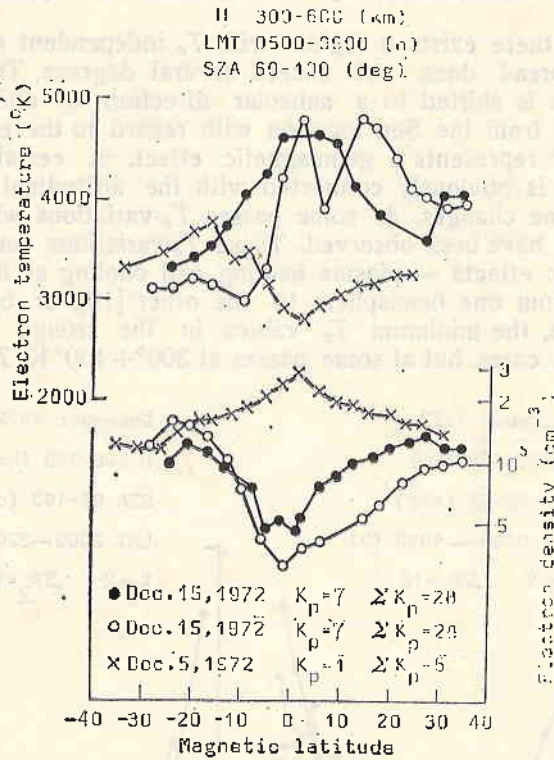


Fig. 4

Fig. 3b shows that a quick decrease of  $T_e$  occurs at sunset. This decrease is related to the fact that in contrast to the midlatitudes, in the equatorial region there is no heat input from the plasmasphere. This means that in the  $\Phi > \pm 20^\circ$  latitudinal region there are no significant sources for electron gas heating after sunset. The  $T_e$  decrease is a peculiarity of the equatorial atmosphere, and this peculiarity takes place at least to  $\Phi \approx 25^\circ$  for altitudes of  $500 \text{ km} \div 600 \text{ km}$ .

The slow decrease of  $T_e$  after  $\Phi = -25^\circ$  when the satellite moves to the north is probably connected with the altitudinal decrease. Moreover, since  $T_e$  is close to  $T_m$ , a  $T_n$ -decrease of about  $100^\circ \text{K}$  at the transition from  $20^{\text{h}}00^{\text{m}}$  LT and  $\Phi = -30^\circ$  in the summer hemisphere to  $22^{\text{h}}00^{\text{m}}$  LT and  $\Phi = +30^\circ$  in the winter hemisphere (Jacchia-71) plays a certain role.

The behaviour of  $T_e$  and  $n_e$  in the transition time from night to day ( $5^{\text{h}}00^{\text{m}} \div 9^{\text{h}}00^{\text{m}}$  LT, i. e. during the sunrise period and the first hours after it),

is shown on Fig. 4. This behaviour has been established according to Langmuir probe data. The Figure represents the results from three satellite passes — one performed in continuous quiet magnetic period and two passes in a magnetically strongly disturbed period. The main characteristic of these curves is the high  $T_e$  value.  $T_e > 2000^\circ\text{K}$  in quiet conditions over the geomagnetic equator at 500 km and attains  $3800^\circ\text{K}$  in a magnetically disturbed period. Moreover, both in quiet and disturbed periods there exists clearly expressed, up to the smallest details, an inverse proportional dependence between  $T_e$  and  $n_e$ .  $T_e$  considerably exceeds  $T_n$  in the geomagnetic equator region at  $H=400\div 500$  km. Therefore at this time the heat input exceeds the electron cooling by the ions (at these altitudes mainly  $\text{O}^+$ , which decreases sharply). During this time the heat input has already attained the stable day level and after  $2\div 3$  hours (Fig. 3a)  $T_e$  again decreases to values close to  $T_n$ .

The midlatitudes of the northern hemisphere have been crossed by the satellite at the night before sunrise (Fig. 4 —  $\chi > 100^\circ$ ). At that time  $T_e$  should be close to  $T_n < 1000^\circ\text{K}$  (Fig. 3b), because the heating influx from the magnetosphere at the end of the night before sunrise cannot ensure a considerable difference  $T_e - T_n$  [20]. Therefore, the values of  $T_e > 2000^\circ\text{K}$  at midlatitudes in the north hemisphere in the given case are determined by the only significant heating source — the photoelectron flux from the magnetically conjugated region of the ionosphere, which was lit up during the time ( $\chi < 87^\circ$ ).

## Discussion

The time development of the equatorial anomaly for the altitudinal and longitudinal regions examined shows a decay of the equatorial trough after about  $19^{\text{h}}00^{\text{m}}$  LT. It has been found in [6] that over the American continent it is difficult to determine the period of the equatorial anomaly decay because of the appearance of intense  $F$ -spread after  $22^{\text{h}}00^{\text{m}}$ . The beginning of the anomaly decay obtained here clarifies this problem, though only for the altitudinal part examined. In 3a we have shown that the equatorial anomaly for altitudes over 900—1200 km remains during night for the regions around the Brazilian magnetic anomaly. Therefore, a complete clarification of the temporal and spacial conditions for the equatorial anomaly decay calls for measurements in the whole region of the maximal electron concentration of the  $F$ -region.

The deviation of the equatorial trough in the ion density from the geomagnetic equator is connected mainly with the deviations of the real geomagnetic field from the dipole one used in this study.

In the region over the Brazilian magnetic anomaly after sunset an intensification of the irregular structure has been determined which is connected with the ionizing influence of the intense corpuscular fluxes [30]. The electron temperature  $T_e$  in the geomagnetic equator region at altitudes higher than the  $F_2$ -region maximum to at least 600 km during the winter of 1972-1973 for more than 50 days, excluding the several hours near the sunrise period, is close to the temperature of the neutral particles. During the day, in the latitudinal  $T_e$ -variations this decrease takes the form of a trough with a minimum, shifted at  $\approx 5^\circ$  in the subsolar direction and expand-

ing to  $20^\circ \div 30^\circ$  on both sides. During nighttime in the altitudinal interval of 300-500 km  $T_e = T_n$ . Because of the absence of heating sources in the latitudinal variation of  $T_e$ , there exists a plateau  $T_e = T_n$  up to  $\Phi \approx 40^\circ$ . The deviation from this ratio takes place in these ionospheric regions where at least at one end of the field line, passing over the equator in the examined altitudinal interval, there occurs sunrise.

## References

1. Appleton, E. V. Nature, 157, 1946, 691.
2. Burcard, O. 1950 Proceed. Mixed Commission on Ionosphere, 1951, 145.
3. Maeda, H. Rep. Ionosph. Res., Japan, 9, 1955, 59.
4. Керблай, Т. С. Исследования ионосферы, М., 1960, 5, 74.
5. Rao, V. C. N. J. Geophys. Res., 68, 1963, 2541.
6. Eccels, D., J. W. King. PIEEE, 57, 1969, 1012.
7. Goldberg, R. A. PIEEE, 57, 1969, 1119.
8. Гдалевич, Г. Л., Б. Н. Горожанкин, Й. С. Кутнев, Д. Т. Самарджнев, К. Б. Серафимов. Космические исследования, 11, 1973, 2, 245.
9. Serafimov, K. B., J. S. Kutiev, S. K. Charukov, Ts. P. Dachev, K. J. Gringauz, G. L. Gdalevich, B. N. Gorojankin. Rep., Days of Bulgarian Sci. and Techn., India, 1973.
10. Anderson, D. W. Planet Space Sci., 21, 1973, 421.
11. Dyson, P. L., J. Geophys. Res., 74, 1969, 6291.
12. McClure, J. P., W. V. Manson. J. Geophys. Res., 78, 1973, 7431.
13. Sagalin, R. G., M. Smiddy, M. Aboned. J. Geophys. Res., 79, 1974, 4255.
14. Гершман, Б. Н. Динамика ионосферной плазмы. М., Наука, 1974.
15. Грингауз, К. Й., К. Б. Серафимов, К. Г. Шмисловски, Я. Шмилауер. Космические исследования, 11, 1973, 1, 95.
16. Бишов, К., Г. Л. Гдалевич, В. С. Губски, Я. Д. Дмитриева, Г. З. Циммерман. Космические исследования, 11, 1973, 2, 267.
17. Афонин, В. В., Г. Л. Гдалевич, К. Й. Грингауз, Я. Кайнарова, Я. Шмилауер. Космические исследования, 11, 1973, 2, 254.
18. Серафимов, К. Б., С. К. Чапкьнов. Военна техника, 7, 1973, 4, 1618.
19. Hanson, W. V., A. S. Nagy, R. T. Moffet. J. Geophys. Res., 78, 1973, 751.
20. Шмилауер, Я., К. Й. Грингауз, В. В. Афонин. Геомагнетизм и аэрономия, 15, 1975, 4 (в печати).
21. McClure, J. P. J. Geophys. Res., 74, 1969, 289.
22. McClure, J. P. J. Geophys. Res., 76, 1971, 3106.
23. McClure, J. P., V. E. Troy. J. Geophys. Res., 76, 1971, 4534.
24. Brace, L. H., V. M. Reddy. J. Geophys. Res., 70, 1965, 5783.
25. Bauer, L. P. Planet. Space Sci., 18, 1970, 1447.
26. Clark, D. H., W. J. Raitt, A. P. Willmore. J. Atmos. Terr. Phys., 35, 1973, 63.
27. Hopkins, H. D. Planet. Space Sci., 20, 1972, 2093.
28. Пономарев, В. Н. Космические исследования, 9, 1971, 6, 878.
29. Rao, V. C. N. Scientific Report No 30, NPL, 1966.
30. Knudsen, W. C. J. Geophys. Res., 73, 1968, 841.



## Измерение ионной концентрации в экваториальном районе

К. Б. Серафимов, И. С. Кутиев, Й. Ф. Арсов, Ц. П. Дачев, Г. А. Станев,  
Г. Л. Гдалевич, В. В. Афонин, В. Губский, В. Озеров, Я. Шмилауер

(Резюме)

По полученным данным от сферичных ионных ловушек и от радиочастотного электронного зонда, которые были монтированы на спутнике „Интеркосмос-8“, в работе исследуется поведение экваториальной аномалии в послеполуденные и вечерние часы, на высотах 300—500 км. Результаты, полученные в долготном интервале  $150^{\circ}$ — $0^{\circ}$ , показывают аномальное распределение ионной концентрации, что тесно связано с реальным геомагнитным полем. В послеполуденные часы наблюдается ясно выраженное двухмаксимумное распределение. В районе Бразильской магнитной аномалии северный максимум выражен сильнее и смещается к магнитному экватору. В вечерние часы (от  $18^{\text{h}}30^{\text{m}}$  до  $21^{\text{h}}08^{\text{m}}$  местного времени) наблюдается исчезновение двухмаксимумного распределения для того же долготного интервала. В районе Бразильской магнитной аномалии наблюдаются крупномасштабные ионосферные неоднородности. Электронная температура, измеренная при вышеуказанных условиях, не различается сильно от температуры нейтральной атмосферы в широтном районе  $\pm 40^{\circ}$ .